Diamond & Related Materials 18 (2009) 433–437

Contents lists available at ScienceDirect

Diamond & Related Materials

journal homepage: www.elsevier.com/locate/diamond

Effects of nitrogen-doping on the microstructure, bonding and electrochemical activity of carbon nanotubes

Y.G. Lin [a], Y.K. Hsu [b], C.T. Wu [b], S.Y. Chen [a], K.H. Chen [b,c], L.C. Chen [c,*]

[a] Department of Materials Science and Engineering, National Chiao Tung University, Hsinchu 30010, Taiwan
[b] Institute of Atomic and Molecular Sciences, Academia Sinica, Taipei 10617, Taiwan
[c] Center for Condensed Matter Sciences, National Taiwan University, Taipei 10617, Taiwan

ARTICLE INFO

Available online 10 September 2008

Keywords:
Carbon nanotubes
Electron-transfer
Nitrogen-doping

ABSTRACT

Vertically aligned carbon nanotubes produced with in-situ doping of nitrogen (CN_x NTs) during chemical vapor deposition exhibit unique structural and electrochemical properties, which are strongly correlated with their nitrogen (N) doping level. In this work, the effects of N-doping on CN_x NTs have been systematically investigated via microstructure and bonding studies, electron-transfer (ET) behaviors, and subsequent electrochemical deposition of catalyst. The CN_x NTs doped with an optimal N level, while showing a nearly reversible ET behavior, in fact exhibit uniform and high density of surface defects. These surface defects are desirable for further modification and/or nucleation of catalytic particles on the surface of CN_x NTs to form a composite electrode for electrochemical energy device applications such as fuel cells and capacitors.

1. Introduction

Carbon nanoscience and nanotechnology have been developed very rapidly over the past decade since the discovery of carbon nanotubes (CNTs). Miniaturization of electronic and electrochemical (EC) devices using the single-walled CNTs has been demonstrated [1–3]. Meanwhile, the remarkable structure of CNTs offers attractive scaffolds for further anchoring of nanoparticles (NPs) and biomolecules, which is highly desirable for energy conversion/storage and molecular sensing applications [4–15]. For these applications, surface modification of the CNTs or attaching functional groups on the sidewall become a key issue. In particular, surface modification offers an opportunity to improve the EC reactivity of CNTs through facilitating an efficient route for their electron-transfer (ET) kinetics with ambient species or specific biomolecules. Therefore, understanding the ET behavior between the CNT surface structures and the active entities are essential.

Several approaches such as acid-based wet-chemical oxidation, amidation, or esterification, diimide activation and solubilization of CNTs have been adopted to effectively functionalize CNTs surface [16,17]. Despite that many solutions to modify CNTs are available, simple and reliable process to achieve such goal is still lacking. In the past we have introduced heteroatom dopant such as nitrogen (N) *in-situ* during the CNT growth and found it effective not only to change the atomic structure of the CNTs into bamboo like [18], but also to improve their electrochemical (EC) performance down the road [10]. Although many reports on nitrogen doped carbon nanotubes (CN_x NTs) are available in the literature [18–21], the role of N-doping in carbon nanotube and its resultant functionality is still not clearly understood.

In this paper, systematic studies on the effect of N incorporation in CNTs on the morphology, microstructures, electronic states, and electrochemical properties have been carried out. CN_x NTs with different nitrogen content have been produced using a simple *in-situ* nitrogen doping in a microwave plasma enhanced chemical vapor deposition (MPECVD) reactor [18]. Comparative studies to correlate the nitrogen content, microstructure, electronic structure, and EC performance of the CN_x NTs have been carried out. Subsequent loading of Pt NPs on the CN_x NTs to study the correlation of N doping with surface defect density and distribution has been carried out.

2. Experimental

For the synthesis of the CN_x NTs, an iron catalyst layer was deposited on Ti/Si substrates by ion beam sputtering prior to the NT growth step. Then CN_x NTs were grown on the precoated substrates by MPECVD method, which has been reported in our previous paper [18]. For Pt NPs deposition, a potential of −0.1 V vs Ag/AgCl in 0.5 M H_2SO_4 and 0.0025 M H_2PtCl_6 mixture solutions was performed for 15 s. Other details for the electrochemical deposition process are reported by Quinn and co-workers [22]. For microstructure and bonding investigation, a JEOL 6700 FESEM, HRTEM (JEOL-400 EX) and Microlab 350 XPS were used. Raman spectra were obtained with a Jobin Yivon Labram HR800 spectrometer with a 514.5 nm argon ion

---

* Corresponding author.
E-mail address: chenlc@ntu.edu.tw (L.C. Chen).

0925-9635/$ – see front matter © 2008 Elsevier B.V. All rights reserved.
doi:10.1016/j.diamond.2008.09.009

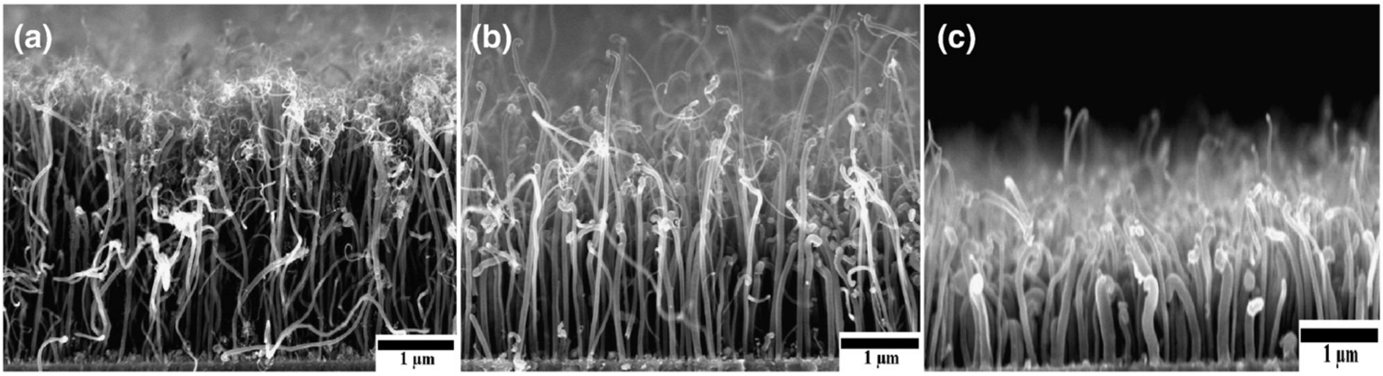

Fig. 1. Cross-sectional SEM images of the vertically aligned CNTs synthesized at different flow rate of N_2: (a) 0, (b) 80, and (c) 120 sccm.

laser. Cyclic voltammogram (CV) and AC impedance were recorded by using Solartron 1470E multichannel potentiostat system.

3. Results and discussion

3.1. Microstructure and bonding of nitrogen-doped carbon nanotubes

Fig. 1 shows the cross-sectional scanning electron microscopy (SEM) images of the vertically aligned CNTs synthesized using different flow rate of N_2 gas but otherwise identical growth parameters. The diameters of the CNTs thus produced are in the range of 20–50 nm with an approximate length of 2–4 µm. Bamboo-like structure of the CN_x NTs is observed, as reported in our previous paper [18]. However, as the N_2 gas flow is higher than 80 sccm the average diameter of the CNTs goes beyond 100 nm with a reduced length of 1–2 µm. This may be attributed to the higher growth temperature at higher N_2 flow rate, which is deviated from the nominal growth condition.

The Raman spectra of the CN_x NTs prepared under different nitrogen flow rate are presented in Fig. 2. The 1350 cm^{-1} peak (D band) in Fig. 2(a) corresponds to the disorder-induced feature due to the finite particle size effect or lattice distortion, while the 1580 cm^{-1} peak (G band) corresponds to the in-plane stretching vibration mode E_{2g} of single crystal graphite [23]. A D′ band around 1620 cm^{-1} at the shoulder of the G band is attributed to the symmetry breaking duo to the microscopic sp^2 crystallite size [24]. The D-band position and the ratio of the D- and G-band integrated intensities as a function of N_2 flow rate are depicted in Fig. 2(b) and (c), respectively. As the N_2 flow rate increases from 0 to 40 sccm the position of the D band up-shifts slightly and eventually down-shifts over 40 sccm nominal N_2 flow rate. In contrast, the position of the G band does not show clear dependence on the N_2 flow rate. Interestingly, the intensity ratio $I(D)/I(G)$ increases strongly as the N_2 flow rate is increased to 40 sccm and also decreases above the 40 sccm optimal flow rate. In principle, the $I(D)$ increases rapidly as a result of the enhanced defect density. Therefore, the up-shift of the D band and the

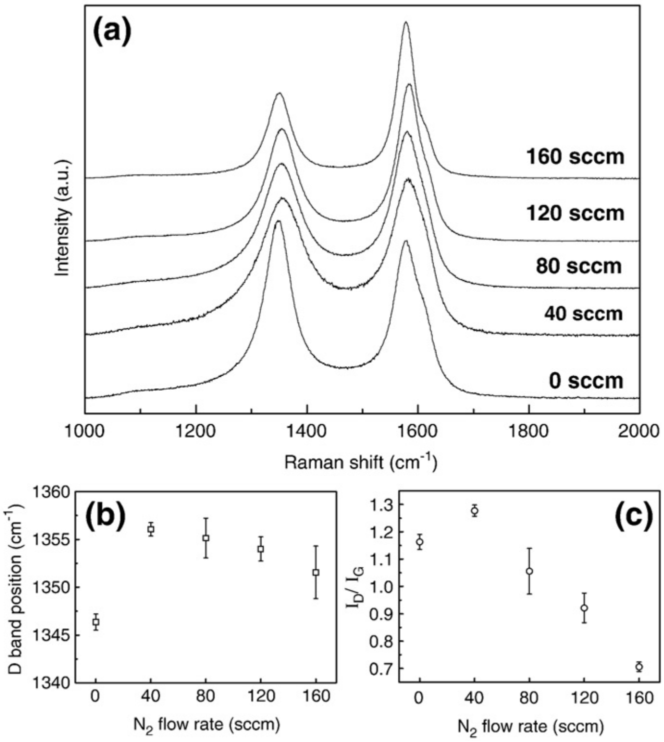

Fig. 2. (a) Comparison of the peak intensities and the full width at half maximum (FWHM) of the first-order Raman spectra for the vertically aligned CN_x NTs prepared with different N_2 flow rate during growth. (b) D-band position as a function of N_2 flow rate. (c) I_D/I_G as a function of N_2 flow rate.